Turkish Journal of Earth Sciences (Turkish J. Earth Sci.), Vol. 18, 2009, pp. 511–528. Copyright ©TÜBİTAK
doi:10.3906/yer-0712-1 First published online 17 August 2009

Geochemistry of the Middle Miocene Collision-related Yamadağı (Eastern Anatolia) Calc-alkaline Volcanics, Turkey

TANER EKİCİ[1], MUSA ALPASLAN[2], OSMAN PARLAK[3] & ALİ UÇURUM[1]

[1] Cumhuriyet University, Department of Geological Engineering, TR–58140 Sivas, Turkey
(E-mail: tanere@cumhuriyet.edu.tr)
[2] Mersin University, Department of Geological Engineering, TR–33343 Mersin, Turkey
[3] Çukurova University, Department of Geological Engineering, TR–01330 Adana, Turkey

Received 07 December 2008; revised typescript received 08 January 2009; accepted 04 March 2009

Abstract: Major, trace element and K-Ar age determinations are reported for a suite from the Yamadağı volcanics in the Eastern Anatolia. The exposed rocks mainly consist of medium-potassium calc-alkaline basaltic andesites, andesites and dacites. Petrographical data exhibit disequilibrium mineral textures, such as resorption of the ferromagnesian phases, clinopyroxene-mantled orthopyroxene, and sieve-textured plagioclases. The Yamadağı volcanics have a calk-alkaline character, and trace element characteristics exhibit that the volcanics resemble subduction zone volcanics and/or volcanics assimilated by continental crust. K/Ar age determinations show that the Yamadağı volcanics were formed during the 12 ± 0.5 – 15 ± 0.5 Ma time interval. Geochemical characteristics of these volcanics can be attributed to complex petrogenetic processes, including magma mixing and crustal assimilation along with fractional crystallization.

Key Words: calc alkaline, volcanics, collision, Eastern Anatolia, Turkey

Çarpışmayla İlişkili Orta Miyosen Yaşlı Yamadağ (Doğu Anadolu) Kalkalkalin Volkanizmasının Jeokimyası

Özet: Doğu Anadolu'daki Yamadağı volkaniklerinden ana, eser element ve K-Ar yaş determinasyonları yapılmıştır. Yamadağı volkaniklerindeki kayaçlar ortaç potasyumlu kalkalkalin bazaltik andezitler, andezitler ve dasitlerden oluşmaktadır. Petrografik olarak elek dokulu plajiyoklaz, ortopiroksenler tarafından mantolanmış klinopiroksenler, resorbe olmuş ferromagnezyan fazlar ve birbirleriyle dengede olmayan mineral toplulukları içermektedir. Kalkalkalin karakterdeki Yamadağı volkanitlerinin iz element karakteristikleri bu volkanitlerin dalma-batma zonu ve/veya kıtasal kabuk tarafından kirletilmiş volkanitlere benzeştiğini göstermektedir. K/Ar yaş tayinleri Yamadağı volkanitlerinin 12 ± 0.5 – 15 ± 0.5 My yaş aralığında oluştuğunu göstermektedir. Yamadağı volkanitlerinin jeokimyasal karakteristikleri bu volkanitlerin evriminde fraksiyonel kristallenmenin yanı sıra magma karışımı ve kabuksal bulaşma süreçlerinin etkin olduğunu göstermektedir.

Anahtar Sözcükler: kalkalkalin, volkanikler, çarpışma, Doğu Anadolu, Türkiye

Introduction

Anatolia (Turkey) is tectonically complex because of the involvement of three major tectonic plates: Arabia and Africa in the south and Eurasia in the north. The Neotectonic evolution of Turkey reflects the interaction between these plates and the minor Anatolian plate (Şengör & Yılmaz 1981; Şengör *et al.* 1985; Dewey *et al.* 1986; Figure 1). The northward motion of the African and Arabian plates triggered subduction in Eocene–Miocene times, followed by diachronous collision along the Bitlis suture zone (e.g., Şengör & Yılmaz 1981). Therefore, geodynamic models suggest that the Anatolian plate was deformed as a result of the collision of the Eurasian

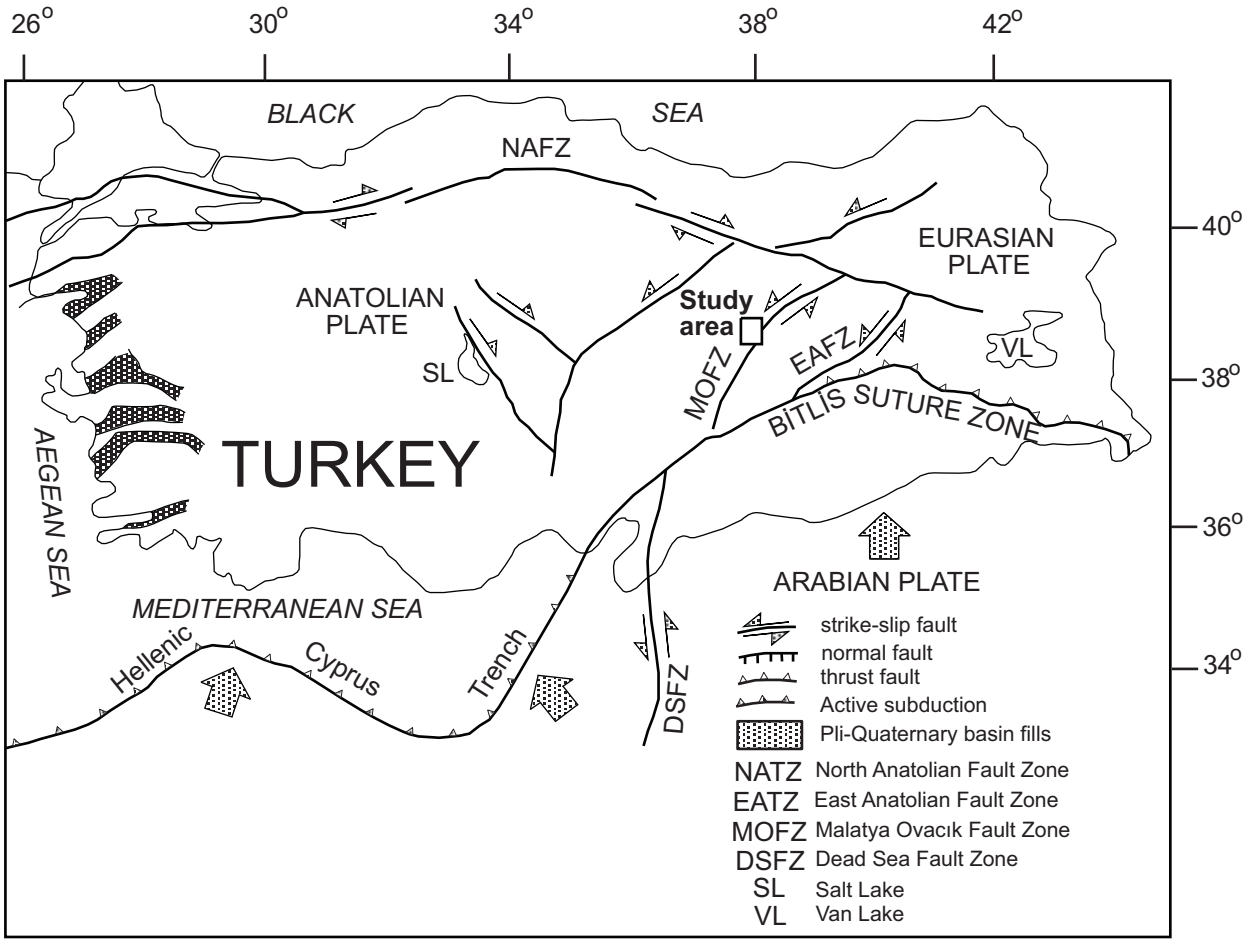

Figure 1. Neotectonic structural elements of Turkey and location of the study area (modified after Koçyiğit *et al.* 2001).

and Arabian plates along the Bitlis suture zone (McKenzie 1972; Şengör 1980). There is no consensus on precisely when collision between the Eurasian and Arabian plates began. The age estimates of collision range from 12 Ma, based on stratigraphic discontinuities in Eastern Anatolia (Şengör & Yılmaz 1981) and the beginning of collision-related volcanism (Pearce *et al.* 1990), to 20 Ma, based on the convergence rate of the two plates (Dewey *et al.* 1986). This collision, which occurred during the Neogene period, resulted in shortening of Eastern Anatolia (McKenzie 1972; Şengör & Kidd 1979; Şengör *et al.* 1985) as well as younger extensional tectonics (Şengör & Kidd 1979; Şengör 1980; Yılmaz 1990).

Extensive volcanic activity took place in Eastern Anatolia during the neotectonic period (Middle Miocene to present), as a result of which volcanic rocks were erupted over large areas. Calc-alkaline volcanic rocks were produced when the compressional regime led to crustal thickening. Calc-alkaline volcanics, which have chemical compositions with subduction signatures inherited from pre-collision subduction events (Notsu *et al.* 1995), were succeeded by alkaline volcanics during the final stage of the compressional regime (Yılmaz 1990).

Many researchers have discussed the origin, age and tectonic settings of these volcanic rocks (Lambert *et al.* 1974; Innocenti *et al.* 1976; Şaroğlu &

Yılmaz 1984; Gülen 1984; Tokel 1984; Alpaslan & Terzioğlu 1996; Keskin *et al.* 1998; Yılmaz *et al.* 1998; Buket & Temel 1998).

In this paper, we present geochemical characteristics and K-Ar data on lavas from the Yamadağı volcanism in the Eastern Anatolia. The origin, evolution and tectonic significance of these volcanics are then discussed.

Geological Setting

The study area is located in central-eastern Anatolia (north of Malatya, Figure 1) and is a part of the region that is under approximately north–south and NNE–SSW shortening, related to the collision between the Anatolian and Arabian plates along the Bitlis suture zone (Bozkurt 2001). The eastern part of Anatolia has experienced intra-continental convergence (McKenzie 1969) that resulted in crustal thickening and uplift (Şengör & Kidd 1979), as a direct result of the collision between Arabian and Anatolian plates and extrusion of collision related volcanics (Pearce *et al.* 1990; Yılmaz *et al.* 1998; Ekici 2003). This compressional tectonic regime was replaced by a new compressional-extensional tectonic regime by early Pliocene time following continental collision (Koçyiğit *et al.* 2001). This has resulted in the generation of intracontinental strike-slip faults, namely the North Anatolian and East Anatolian faults (Figure 1). Structural elements of the study area are dominated by a left-lateral strike-slip fault zone, the Malatya-Ovacık fault zone, which has been suggested as the boundary between the Anatolian and Arabian plates (Figures 1 & 2; Westaway & Arger 2001). Based on existing geological studies, three lithostratigraphic units are distinguished within the Lower Miocene–Quaternary (Alpaslan & Terzioğlu 1996; Ekici 2003; Figures 2 & 3). The Yamadağı volcanics consist of intermediate to acidic or silicic lava flows, and their pyroclastic derivatives cover large areas and rest on the Lower Miocene limestones (Figure 2; Alpaslan 1987; Ekici 2003). The age of these volcanics varies from 11.99 ± 0.49 to 14.82 ± 0.57 Ma (Table 1), representing middle to late Miocene ages based on K/Ar geochronology. Pliocene units are represented by lacustrine sediments (Figure 2).

Petrography

Silica and total alkalis (Na_2O+K_2O) were used to classify the rocks on the TAS diagram of Le Maitre *et al.* (1989) (Figure 3). The composition of the volcanic rocks ranges from basaltic andesite to dacite on this diagram (Figure 3).

Basaltic andesites are grey and greyish brown and have a hypocrystalline-porphyritic-pylotaxitic texture. They contain olivine, clinopyroxene, plagioclase and scarce hornblende phenocrysts. Their groundmass consists of plagioclase, olivine, pyroxene, hornblende and opaque mineral microlites and devitrified glass. Reacted hornblende phenocrysts have occasionally been observed in the basaltic andesites.

Andesites are dark grey to black and have an aphanitic texture. They display a hypocrystalline porphyritic-pylotaxitic texture. Phenocryst and microphenocryst phases in the andesites include plagioclase, clinopyroxene, orthopyroxene, hornblende, apatite and opaque minerals. The groundmass also contains palagonitizated volcanic glass.

Dacites are dark-grey and have a hypo-hyaline porphyritic texture. They consist of plagioclase, clino- and ortho-pyroxene and either green or reddish brown hornblende phenocrysts. Their groundmass comprises plagioclase microlites, pyroxene and apatite microphenocrysts, opaque minerals and volcanic glass. Occasional, millimetre-sized crystal-rich enclaves occur in the dacites (Figure 4A). The microlitic nature of these enclaves possibly indicates that they are chilled blobs of basic magma.

Olivine occurs as phenocrysts and microphenocrysts in the basaltic andesites and andesites, sometimes these are penetrated by microcrystalline groundmass (Figure 4B). Some olivine phenocrysts are embayed and olivine also occurs as resorbed phenocrysts in the basaltic andesites. Olivine also was observed as xenocrysts mantled by orthopyroxene in the dacites (Figure 4C).

Clino- and ortho-pyroxenes are found in all rock types as phenocrysts and microphenocrysts. Clinopyroxene is most common in the basaltic andesite whereas orthopyroxene is more prevalent in

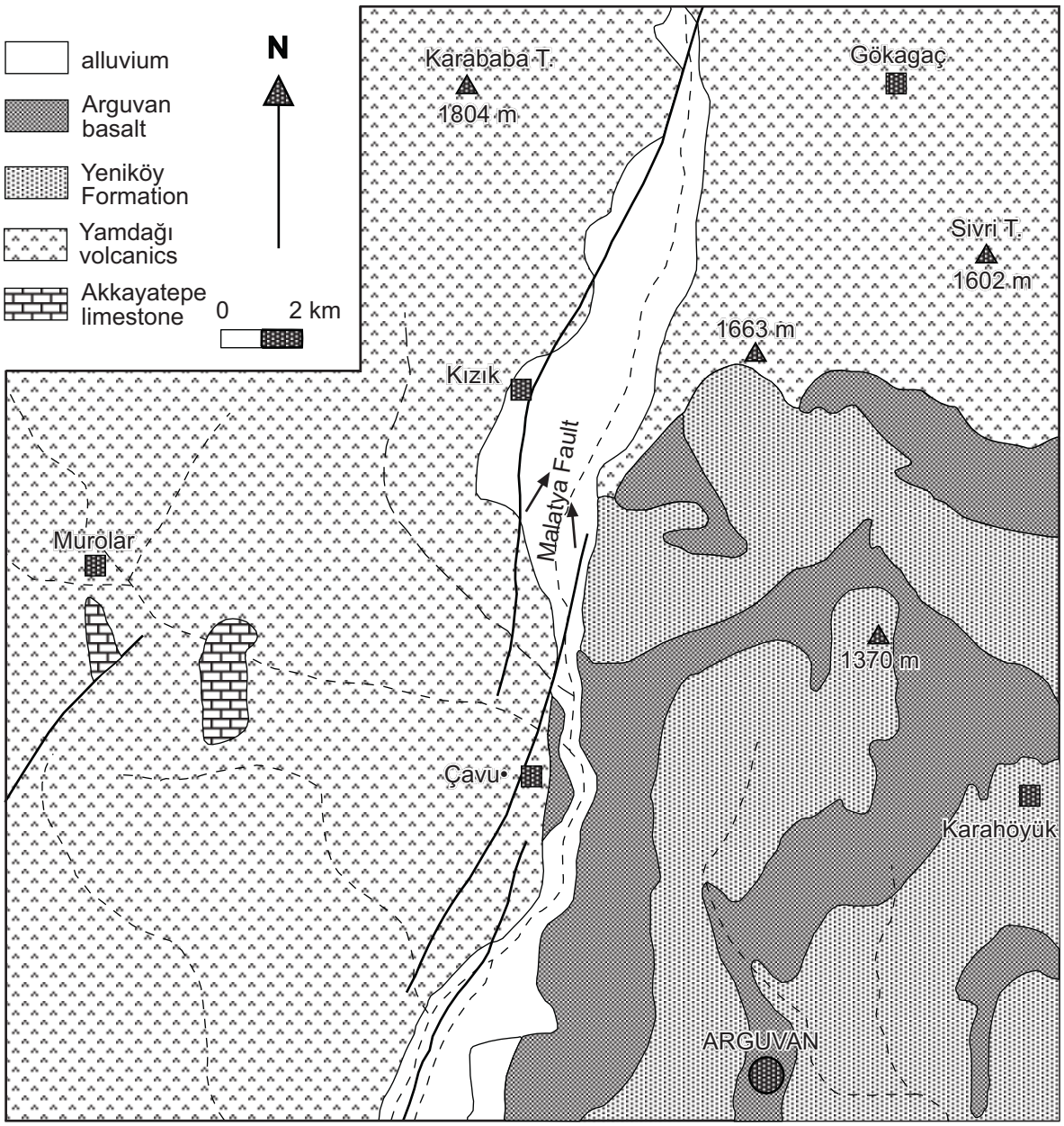

Figure 2. Simplified geological map of the study area.

the andesites. Occasionally, clinopyroxene cores are mantled by overgrowths of orthopyroxene in basaltic andesites (Figure 4D). Some clinopyroxene phenocrysts in the andesites have abundant inclusions of groundmass material in the core (Figure 4E) and the others have embayed margins suggesting resorption (Figure 4F). Orthopyroxene also occurs in glomeroporphyritic aggregates with plagioclase and Fe-oxides and in reaction rims around olivine phenocrysts (Figure 4C).

Plagioclase phenocrysts in the Yamadağı volcanics show clear evidence of multiple origins and periods of dissolution and growth. Based on textural criteria, plagioclase phenocrysts can be identified as one of three types: (a) unsieved, with no dissolution texture, (b) sieve-cored, where the cores are riddled

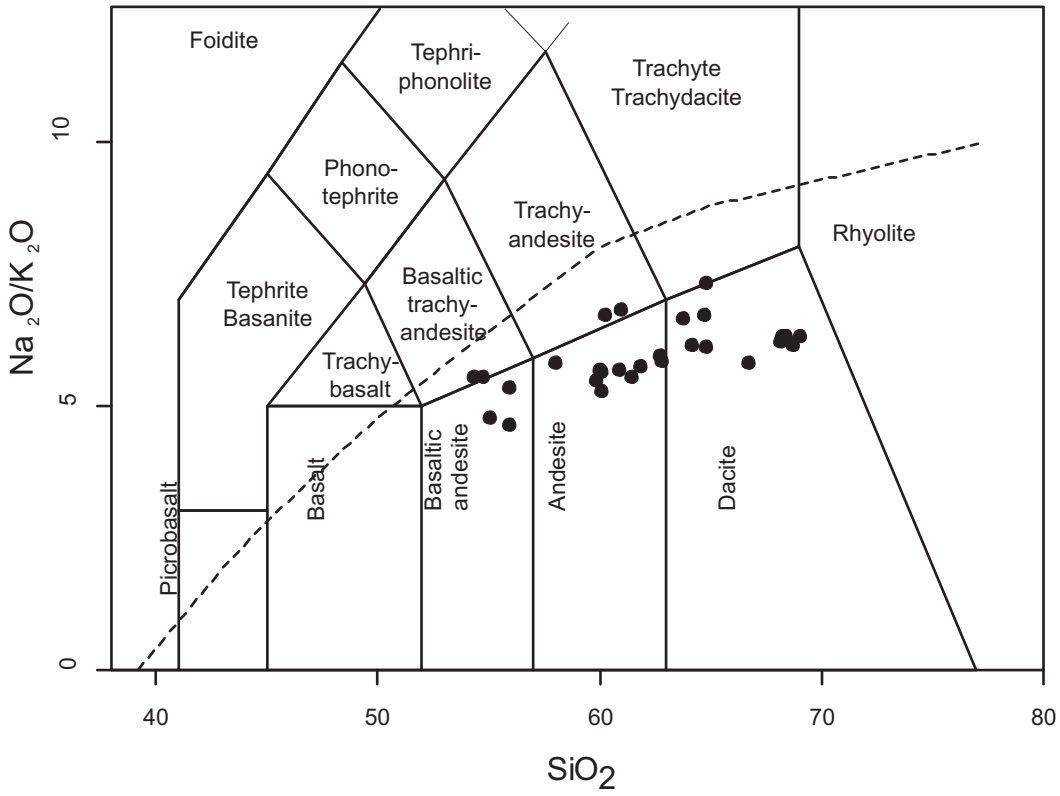

Figure 3. Total alkali-silica nomenclature diagram (Le Bas *et al.* 1986) for the Yamadağı volcanics. Dividing line between alkaline and subalkaline fields after Irvine & Barager (1971).

with glass and overgrown with clear rims, and (c) sieve-ringed, where a clear core is mantled by a resorption zone followed by a clear rim (Figure 4G).

Amphibole occurs as scarce dark reddish brown phenocrysts, which are observed as reacted phenocrysts. They typically have thin rims of fine-grained plagioclase, pyroxene and Fe-Ti oxide (Figure 4H). This feature probably reflects volatile loss during ascent of magma in conduits (Rutherford & Hill 1993). Reacted amphibole phenocrysts are partially replaced by acicular pyroxene and fine-grained oxide minerals [magnetite?]. Amphibole phenocrysts and microphenocrysts with a yellowish-green to green pleochroism are common in the dacites. These amphibole phenocrysts have abundant inclusions of groundmass material in the cores (Figure 4I).

Table 1. K/Ar age (Ma).

Sample	Rock name	Grain size	^{40}Ar radius (ccSTP/g)	^{40}Ar radius (%)	K (%)	K-Ar Age (Ma)
AR-38	Dacite	90-250 μ	1.171×10^{-6}	55.5	2.503	11.99 ± 0.49
AR-40	Dacite	250-400 μ	7.560×10^{-7}	66.3	1.424	13.61 ± 0.53
AR-78	Andesite	<90μ	5.827×10^{-7}	48.1	1.073	13.91 ± 0.59
AR-100	Dacite	90-250 μ	8.198×10^{-7}	53.1	1.461	14.37 ± 0.59
AR-68	Dacite	250-400 μ	8.731×10^{-7}	72.2	1.509	14.82 ± 0.57

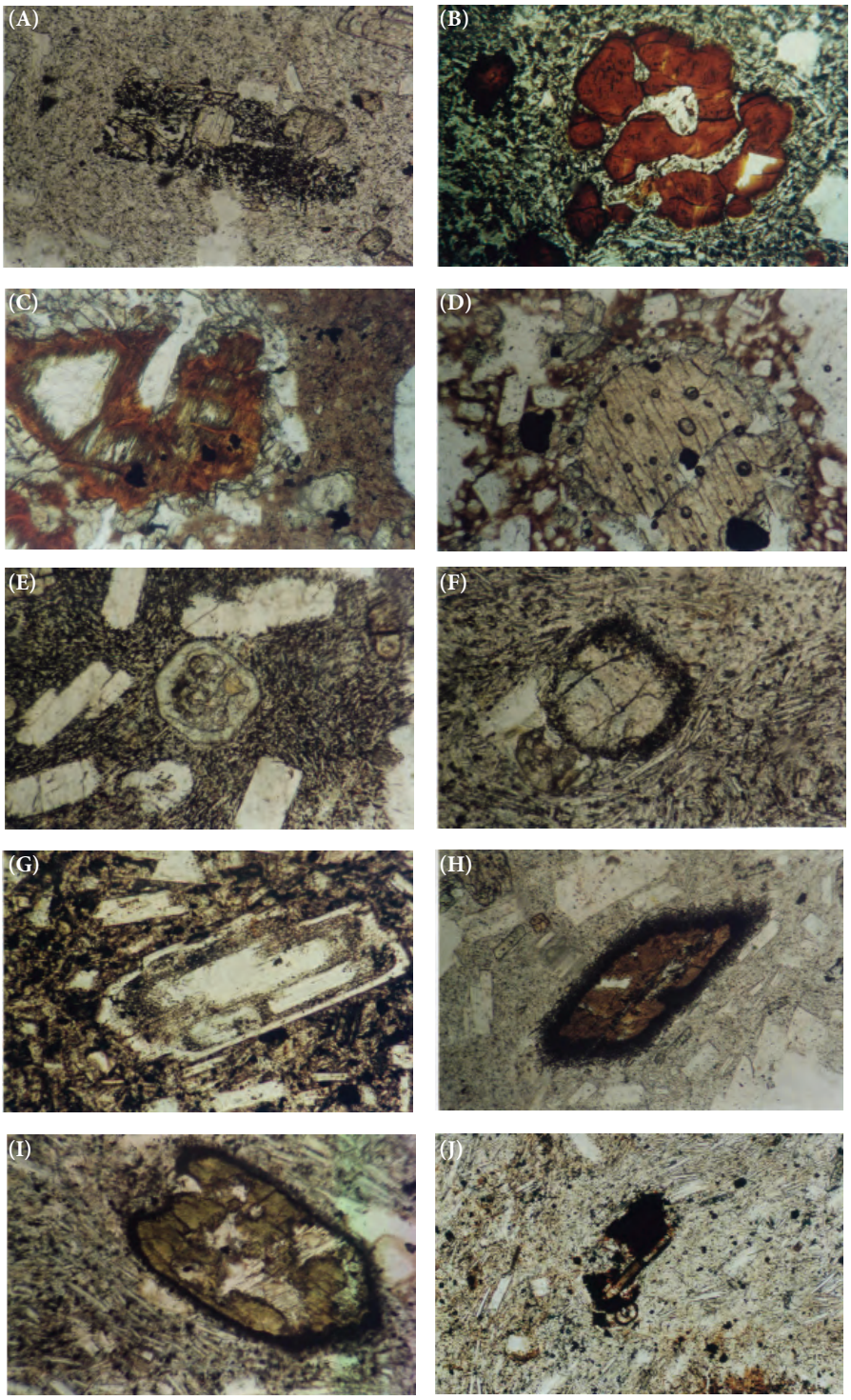

Figure 4. **(A)** Crystal-rich enclave in dacite, **(B)** embayed olivine crystal in basaltic andesite, **(C)** olivine mantled by orthopyroxene, **(D)** clinopyroxene mantled by orthopyroxene, **(E)** groundmass inclusions in clinopyroxene, **(F)** clinopyroxene indicating resorption, **(G)** sieve-textured plagioclase, **(H)** amphibole with thin rims of fine-grained plagioclase, pyroxene and Fe-Ti oxide, **(I)** amphibole with abundant groundmass inclusions in the core, **(J)** dusty apatite microphenocryst in dacite.

Apatite is an accessory phase in the Yamadağı volcanics. It occurs mostly as microphenocrysts in the dacites (Figure 4J). These microphenocrysts are dusted with fine, brown specks and are interpreted to be apatite grains xenocrysts.

Analytical Techniques

Rock powders were prepared by removing altered surfaces, crushing and then grinding. Major element abundances were measured on fused discs. Fused discs were prepared by using five parts of lithium tetraborate and one part of rock powder. The mixture was fused in crucibles of 95%Pt and 5%Au at 1150 °C to form a homogenous melt. The melt then was poured into a preheated mold to chill a thick glass disk. Major element analyses were performed at Lausanne University using an X-ray spectrometer using USGS and GEOSTANDARD rock standards. Trace element concentrations were analyzed at ACME laboratories (Vancouver, CANADA) by ICP-MS with better than ± 3% accuracy using dissolved fusion beads.

For the K-Ar dates, the samples were degassed in a conventional extraction system using induction heating and were measured by mass in spectrometric isotope dilution with a ^{38}Ar spike. Potassium determinations were made using standard flame photometric techniques. K and Ar determinations were checked regularly by interlaboratory standards; HD-B1,LP-6,GL-0 and Asia1/65. Atomic constants suggested by Steiger & Jaéger (1977) were used for calculating the radiometric ages. All analytical errors represent one standard deviation (68% confidence level). Details of the instruments, the methods applied and results of calibration have been described by Balogh (1985).

Major- and Trace-element Geochemistry

Major- and trace-element analyses were carried out on twenty-eight Yamadağı samples (Table 2a, b). The volcanic rocks have a wide range of chemical composition with SiO_2 contents ranging between 54% and 70% without a compositional gap, and have been classified on the basis of their alkali and silica contents using the total alkali – SiO_2 diagram (TAS) of Le Bas *et al.* (1986) and K_2O–SiO_2. On the TAS diagram (Figure 3) volcanic rocks with intermediate-acidic and sodic compositions are represented by basaltic andesites, andesites and dacites. The Peccerillo & Taylor (1976) diagram shows that all samples are similar to calc-alkaline rocks, falling within the medium-K series (Figure 5). The volcanic rocks are dominantly characterized by subalkaline trends on the total alkali – silica diagram (Figure 3), and generally show a typical calc-alkaline differentiation trend on an AFM diagram (Figure 6). In the Harker diagrams, as SiO_2 increases, Fe_2O_3, MgO, CaO, TiO_2 and P_2O_5 decrease and K_2O increases (Figure 7). Such negative and positive correlations can be explained by removal of the ferromagnesian phases such as olivine and pyroxene, and apatite. Compatible trace elements such as Co, V and Y show strong negative correlation with increasing SiO_2, whereas incompatible trace elements correlate positively (Figure 7). These major and trace element trends are broadly consistent with plagioclase+pyroxene+Fe-Ti oxides+hornblende, all of which are present as phenocrysts in the Yamadağı volcanics.

Primitive mantle-normalized trace element patterns of the Yamadağı volcanics (Figure 8) are characterized by a Nb-Ta trough and are enriched in incompatible trace elements. Negative and positive Pb anomalies occur in all the rock types of the Yamadağı volcanics (Figure 8).

When compared with the multi-element diagrams of the Yamadağı volcanics, the basaltic andesites (Figure 8) are characterized by a less marked enrichment in Rb, Ba, Th, K, and a negative Nb anomaly. The andesites and dacites display multi-element patterns consistent with their possible derivation from the associated basaltic andesites through crystal fractionation: enrichment in Rb, Th, K and negative anomalies in Ba, Nb, and Ti. The REE patterns of the basaltic andesites (Figure 8a) exhibit enriched light REE but the $(La/Yb)_N$ ratios (7.81) are lower than in the andesites (9.01) and dacites (10.42).

Discussion

Fractional Crystallization

The new data reported in this study indicate that the Yamadağı volcanic rocks have similar petrographical and geochemical features and define typical calc-

Table 2a. Whole-rock major element compositions of the Yamdağı volcanics. Major oxides are given as weight per cent (Fe_2O_3 as total iron, LOI as loss on ignition).

Sample	SiO_2	TiO_2	Al_2O_3	Fe_2O_3	MnO	MgO	CaO	Na_2O	K_2O	P_2O_5	LOI
Ar-17	57.55	1.26	18.38	6.91	0.08	2.62	6.40	4.36	1.39	0.26	0.88
Ar-19	68.14	0.50	16.35	3.23	0.03	1.05	3.85	4.61	1.68	0.14	0.66
Ar-25	55.75	0.87	19.36	7.81	0.16	3.02	7.84	3.68	0.93	0.17	0.38
Ar-34	63.74	0.72	17.01	4.69	0.08	1.32	5.14	4.32	1.76	0.47	0.76
Ar-37	54.60	1.25	17.85	7.60	0.12	4.47	8.21	3.61	1.12	0.24	0.71
Ar-38	63.25	0.86	16.53	4.81	0.08	2.13	4.67	3.66	2.94	0.22	1.04
Ar-40	66.02	0.61	16.87	3.59	0.05	1.24	4.56	4.08	1.67	0.16	1.12
Ar-41	60.48	0.99	17.47	5.83	0.08	1.80	5.37	4.74	2.02	0.33	0.69
Ar-42	64.13	0.79	16.78	4.16	0.07	1.87	4.33	4.08	2.55	0.22	0.62
Ar-45	59.87	1.03	17.27	6.06	0.09	2.56	5.41	4.65	2.01	0.34	0.41
Ar-49	63.98	0.58	17.60	4.56	0.08	0.83	3.58	4.85	2.37	0.25	0.97
Ar-51	54.95	1.18	17.18	8.28	0.12	5.34	6.91	4.14	1.12	0.08	0.21
Ar-53	62.23	0.81	16.31	5.39	0.09	3.16	5.13	3.81	2.09	0.18	0.64
Ar-54	54.17	1.31	17.37	8.62	0.14	4.95	7.25	4.20	1.31	0.33	0.20
Ar-55	59.79	0.85	16.05	6.24	0.09	5.02	5.96	3.85	1.38	0.20	0.45
Ar-58	55.65	1.15	17.62	8.50	0.13	5.47	5.37	4.15	1.16	0.21	0.50
Ar-64	54.66	1.39	18.22	8.28	0.12	3.81	7.48	4.39	1.12	0.29	0.33
Ar-67	62.34	0.76	16.66	4.99	0.08	2.45	5.82	4.13	1.66	0.28	0.81
Ar-68	64.09	0.75	16.88	4.55	0.06	1.56	4.73	4.25	1.77	0.20	1.23
Ar-77	61.04	0.81	17.12	5.23	0.08	3.39	5.99	3.65	1.86	0.18	0.58
Ar-78	59.76	0.99	17.07	6.14	0.08	3.42	6.14	4.16	1.43	0.20	0.62
Ar-80	59.31	0.99	17.08	5.69	0.09	3.94	6.39	3.88	1.52	0.19	0.42
Ar-83	59.84	0.99	17.02	6.12	0.09	3.61	6.17	4.22	1.43	0.20	0.30
Ar-85	67.20	0.48	16.09	3.04	0.05	1.48	3.79	3.68	2.52	0.13	1.29
Ar-86	67.64	0.46	15.98	2.96	0.05	1.46	3.71	3.54	2.51	0.12	1.62
Ar-87	68.25	0.41	15.89	2.87	0.05	1.41	3.57	3.64	2.58	0.12	1.34
Ar-88	61.36	1.05	18.28	5.49	0.09	1.48	5.49	4.51	1.16	0.21	0.94
Ar-89	60.64	1.04	18.39	5.57	0.09	2.20	5.76	4.53	1.13	0.23	0.44
Ar-100	67.99	0.49	16.30	3.07	0.05	1.51	4.02	4.46	1.74	0.13	0.49

Table 2b. Trace element compositions of the Yamadağ volcanics. Trace elements are given as ppm.

Sample	Rb	Ba	Th	Nb	La	Ce	Sr	Sm	Zr	Y	Pr	Nd	Eu	Gd	Tb	Dy	Ho	Er	Tm	Yb	Lu	P	Co	V	Ti	K
Ar-17	36.3	186	5.9	9.8	18.6	36.8	422	3.9	159	21.3	4.4	18.7	1.22	3.87	0.63	3.71	0.76	2.16	0.28	1.82	0.25	6.76	28	138	7552	11539
Ar-19	60.8	220	6	4.8	18	32	312	2.9	146	17.2	3.85	16.9	0.84	2.92	0.44	2.79	0.58	1.56	0.21	1.71	0.24	4.3	23	52	2997	13946
Ar-25	30	195	4.8	5.1	14.1	29.3	329	4	109	25.5	3.63	16.3	1.12	3.69	0.67	4.35	0.91	2.61	0.37	2.79	0.41	5.22	39	135	5215	7720
Ar-34	44.1	457	11.2	29.6	44.6	71.3	547	4.3	218	18.4	7.42	27.6	1.21	3.32	0.58	2.98	0.58	1.73	0.22	1.54	0.25	14.44	21	64	4316	14610
Ar-37	32	140	3	7.4	14.1	29.3	423	3.5	146	23	3.59	16.8	1.26	3.9	0.63	3.76	0.76	2.19	0.34	2.17	0.29	7.37	49	158	7492	9297
Ar-38	73.8	276	7	11.4	19.4	37.8	374	3.2	168	18.8	4.11	17	0.86	3.13	0.47	2.88	0.61	1.64	0.25	1.35	0.25	6.76	30	80	5155	24406
Ar-40	55.6	279	7	7.3	20.8	39.8	305	3.3	151	16.4	4.34	16.7	0.85	2.86	0.44	2.75	0.55	1.48	0.23	1.47	0.2	4.91	24	65	3656	13863
Ar-41	51.6	282	8.4	24.2	30.9	56.3	530	3.9	229	18.2	5.81	22.3	1.14	3.34	0.54	3.06	0.62	1.77	0.26	1.73	0.26	10.14	16	89	5934	16767
Ar-42	78.1	294	9.3	14.5	23.5	39.1	384	3.8	179	19.1	4.71	19.3	0.94	3.24	0.51	3.07	0.66	1.8	0.26	1.7	0.28	6.76	30	74	4735	21168
Ar-45	50.6	275	9.9	22.3	31.9	57.3	557	4.4	229	20.3	6.31	23.7	1.16	3.25	0.58	3.28	0.7	1.85	0.28	1.92	0.31	10.45	25	74	6174	16686
Ar-49	67.3	334	9.6	24.7	29.6	55.5	379	3.8	255	22.2	6.06	22.5	1.1	3.56	0.55	3.83	0.77	2.14	0.34	2.16	0.36	7.68	21	26	3476	19674
Ar-51	77.5	301	10.5	17.9	29.7	55.4	276	4.1	259	21.8	5.77	21.8	0.95	3.56	0.58	3.33	0.77	2.06	0.32	2.11	0.38	2.46	41	127	7073	9297
Ar-53	53.9	166	5.1	6.4	15	31.8	304	3.2	152	19.1	3.58	13.8	0.93	3.04	0.5	3.18	0.64	1.86	0.28	1.77	0.26	5.53	31	96	4855	17350
Ar-54	32.6	190	6.4	13.3	21.9	42.7	441	4.8	180	27.1	5.1	21.6	1.32	4.24	0.74	4.2	0.9	2.71	0.39	2.55	0.35	10.14	41	155	7852	10875
Ar-55	45.7	254	6	8.6	18.9	35.9	352	3.2	143	20.4	4.01	16	0.93	3.31	0.5	3.31	0.66	1.84	0.29	1.85	0.26	6.15	41	110	5095	11456
Ar-58	31.3	120	3.7	7	12.4	26.1	275	3	133	23.8	3.19	12.6	0.96	3.18	0.55	3.83	0.81	2.31	0.35	2.28	0.33	6.45	45	144	6893	9630
Ar-64	20.6	157	3.9	10.5	17.3	33.8	411	4.5	182	30.1	4.27	18.5	1.27	4.77	0.76	4.86	1	2.84	0.39	2.5	0.38	8.91	38	151	8332	9297
Ar-67	56.8	347	9.8	12.2	30.2	53.8	436	3.9	170	19.4	5.66	21.4	0.97	3.03	0.56	3.04	0.64	1.85	0.28	1.98	0.25	8.6	25	92	4555	13780
Ar-68	58.1	346	8.7	9.3	23	45.9	318	4.3	171	18.9	5.15	18.7	0.93	3.58	0.54	3.16	0.62	1.86	0.25	1.83	0.23	6.15	27	71	4496	14693
Ar-77	51.8	200	5.5	7.2	15.8	30.6	391	3.3	144	16.7	3.56	14.4	0.93	2.9	0.45	2.79	0.59	1.54	0.23	1.54	0.24	5.53	39	110	4855	15441
Ar-78	40.6	173	5.9	8.2	15.5	29.8	339	3.2	141	16.9	3.66	15	0.96	3.16	0.45	2.81	0.59	1.62	0.26	1.59	0.22	6.15	31	111	5934	11871
Ar-80	47.6	179	5.2	8.1	15.5	32.5	364	3.4	146	18.6	3.86	15.4	0.94	3.18	0.48	3.09	0.63	1.83	0.26	1.67	0.25	5.84	39	132	5934	12701
Ar-83	43.8	175	6.1	8.8	16.6	31.7	357	3.5	149	20.8	3.79	15.2	1.11	3.51	0.64	3.2	0.6	1.9	0.26	1.87	0.23	6.15	31	127	5934	11871
Ar-85	61.7	181	6.1	4.7	14.5	27.9	297	2.7	129	13.5	3.23	12.9	0.73	2.15	0.36	1.99	0.4	1.21	0.17	1.21	0.19	3.99	37	57	2877	20920
Ar-86	63.6	206	7	4.7	14	29.3	305	2.4	130	13.6	3.19	12.1	0.68	2.16	0.4	2.07	0.42	1.33	0.19	1.29	0.17	3.69	28	55	2757	20836
Ar-87	69.2	228	6.3	4.6	14.1	28.2	305	2.5	128	12.2	3.2	11.5	0.6	2.16	0.33	2.05	0.39	1.13	0.16	1.33	0.19	3.69	31	46	2457	21418
Ar-88	28	324	4.3	8.5	18.3	38.2	371	3.6	146	20.1	4.46	17.2	1	3.36	0.52	3.37	0.69	1.89	0.27	1.87	0.27	6.45	20	78	6294	9630
Ar-89	27.8	313	5.8	9.3	21.3	42.1	415	4.1	170	21.7	4.96	20.6	1.07	3.7	0.63	3.65	0.74	2.08	0.29	2.02	0.35	7.07	28	84	6234	9381
Ar-100	62.7	200	6.1	4.5	14	28.8	302	2.6	137	12.2	3.24	11.6	0.65	2.18	0.36	2.11	0.44	1.11	0.19	1.23	0.17	3.99	21	54	2937	14444

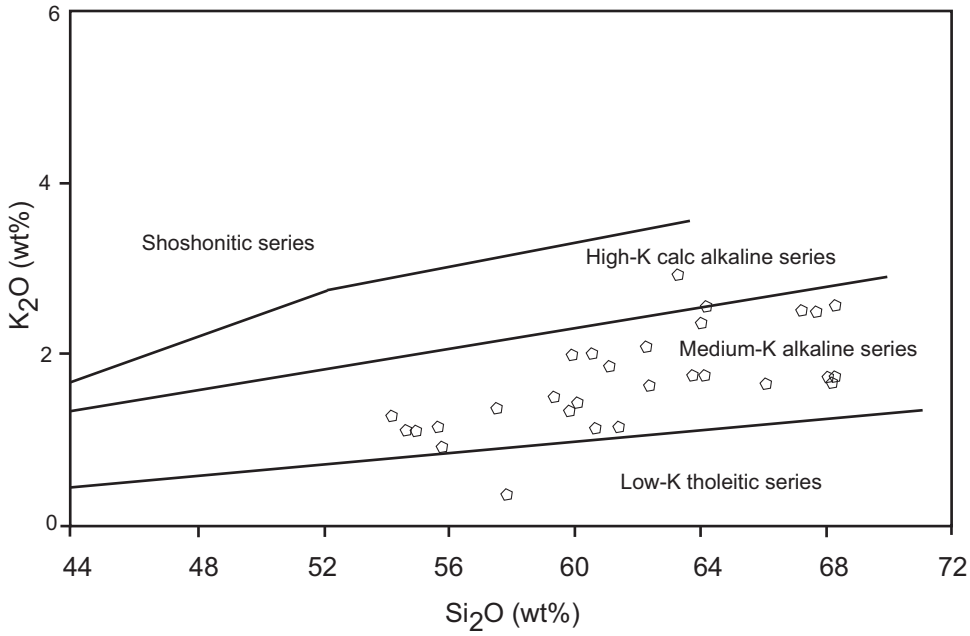

Figure 5. K_2O–SiO_2 diagram (Peccerillo & Taylor 1976) for the Yamadağı volcanics.

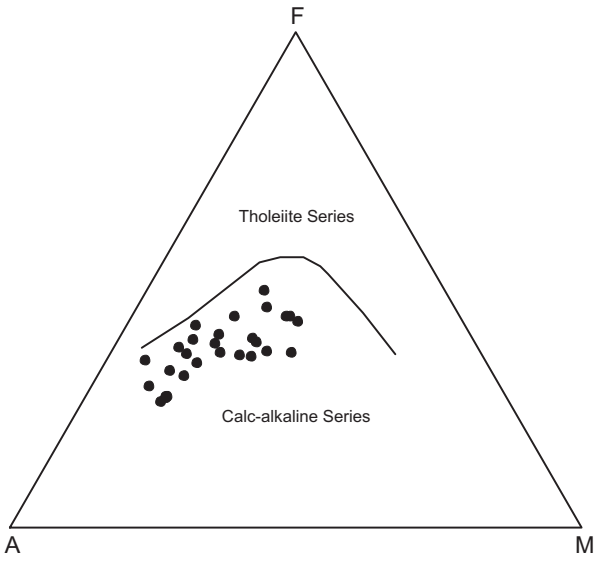

Figure 6. AFM diagram (Irvine & Barager 1971) for the Yamadağı volcanics.

alkaline trends from subalkaline basaltic andesites to dacites. Major- and trace-element abundances vary along continuous trends of decreasing MgO, TiO_2, Fe_2O_3*, CaO, V and Co, and increasing K_2O, Rb, Zr, and Y with increasing SiO_2 (Figure 7). Incompatible (Rb) versus incompatible (K and Y) trace element variations are linear (Figure 9a, b), with trends from low abundances in basaltic andesites towards higher abundances in dacites (Figure 9). Normalized REE patterns of the Yamadağı volcanics form parallel trends, and total REE contents increase from basaltic andesite to dacite (Figure 8). La/Sm data points (Figure 9c) plot along a line, a feature restricted to the process of fractional crystallization (Allegre & Minster 1978).

The above-mentioned characteristics show that the Yamadağı volcanics evolved predominantly through fractional crystallization of the petrographically observed phenocryst assemblage, which is olivine+plagioclase+augite+Fe-Ti oxides in mafic volcanic rocks and plagioclase+two pyroxene+hornblende+Fe-Ti oxides in the acidic rocks.

Crustal Contamination

The chemical data of the Yamadağı Volcanic rocks provide few constraints on whether or not there was significant crustal contamination, particularly because there is no data on the composition of the

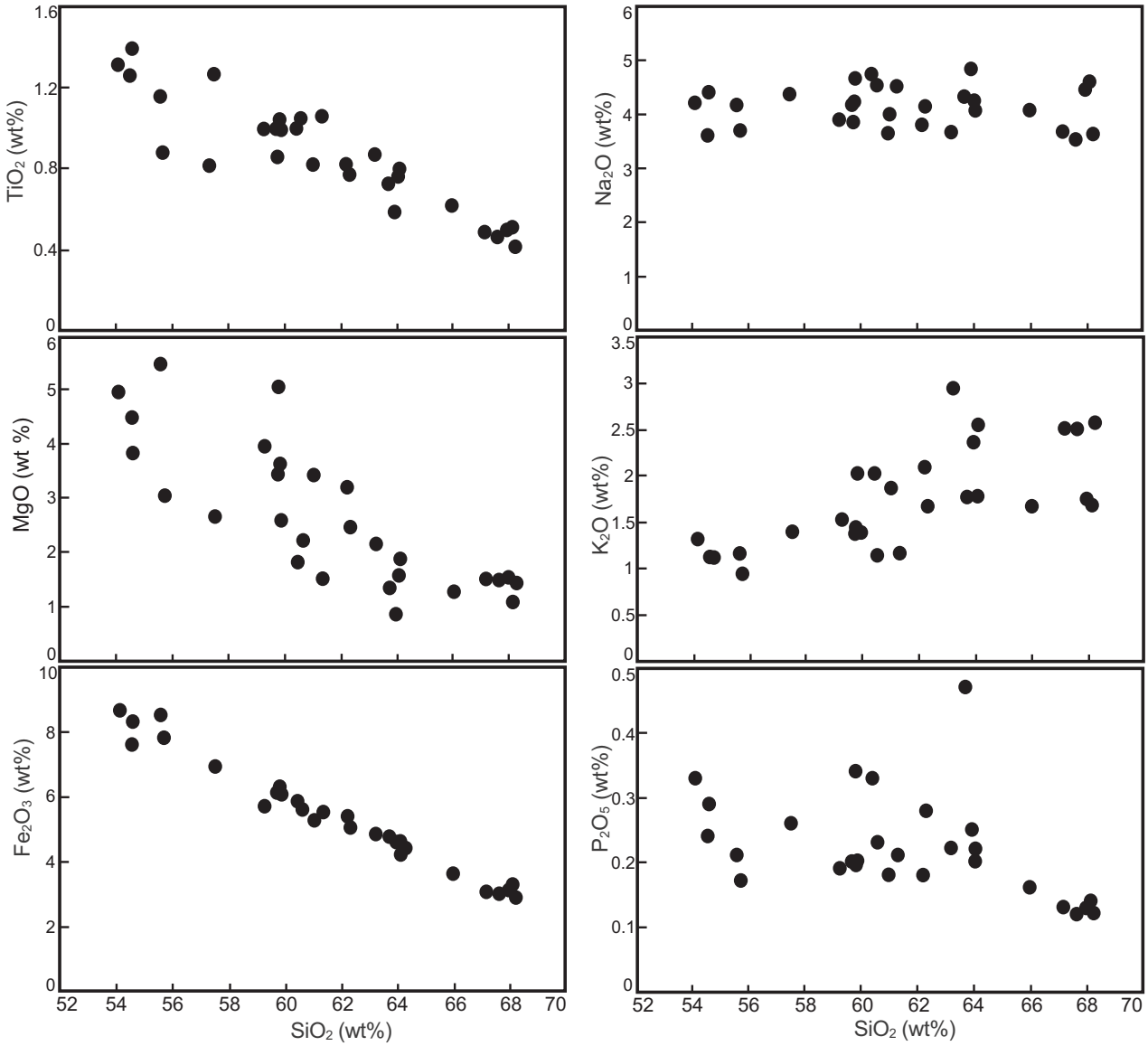

Figure 7. Selected major and trace element variations against SiO_2 content: **(a)** major element; **(b)** trace element.

country rocks that may represent the potential contaminants. However, the LILE (e.g., Rb and K) and Zr are incompatible with respect to the major crystallizing phenocryst assemblage (plagioclase, pyroxene, Fe-Ti oxides) and ratios like K/Rb and Rb/Zr do not significantly change by simple fractional crystallization of this assemblage. Variations in these ratios are preferably related to crustal contamination by assimilation fractional crystallization processes (Davidson *et al.* 1987). Examination of the Yamadağı volcanic rocks shows that, in most of the intermediate volcanic rock samples, it is very significant for both Rb/Zr and K/Rb (Figure 10). Therefore, the role of significant crustal assimilation in the genesis of the intermediate Yamadağı volcanics is unlikely, but cannot be completely ruled out.

In theory, fractional crystallization of magnesian minerals plus plagioclase leads to production that falls within narrow coronal bands characterized by

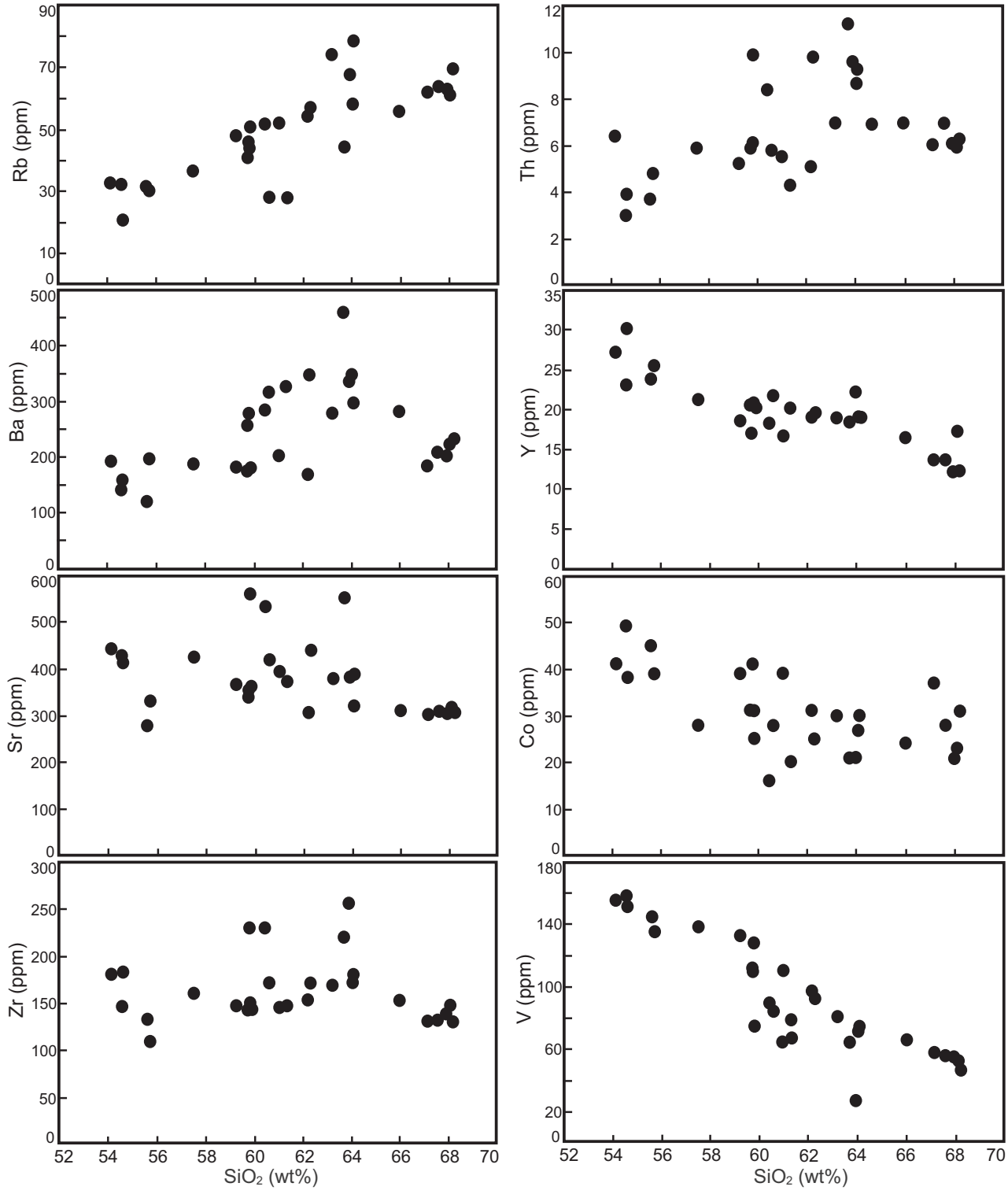

Figure 7. Continued.

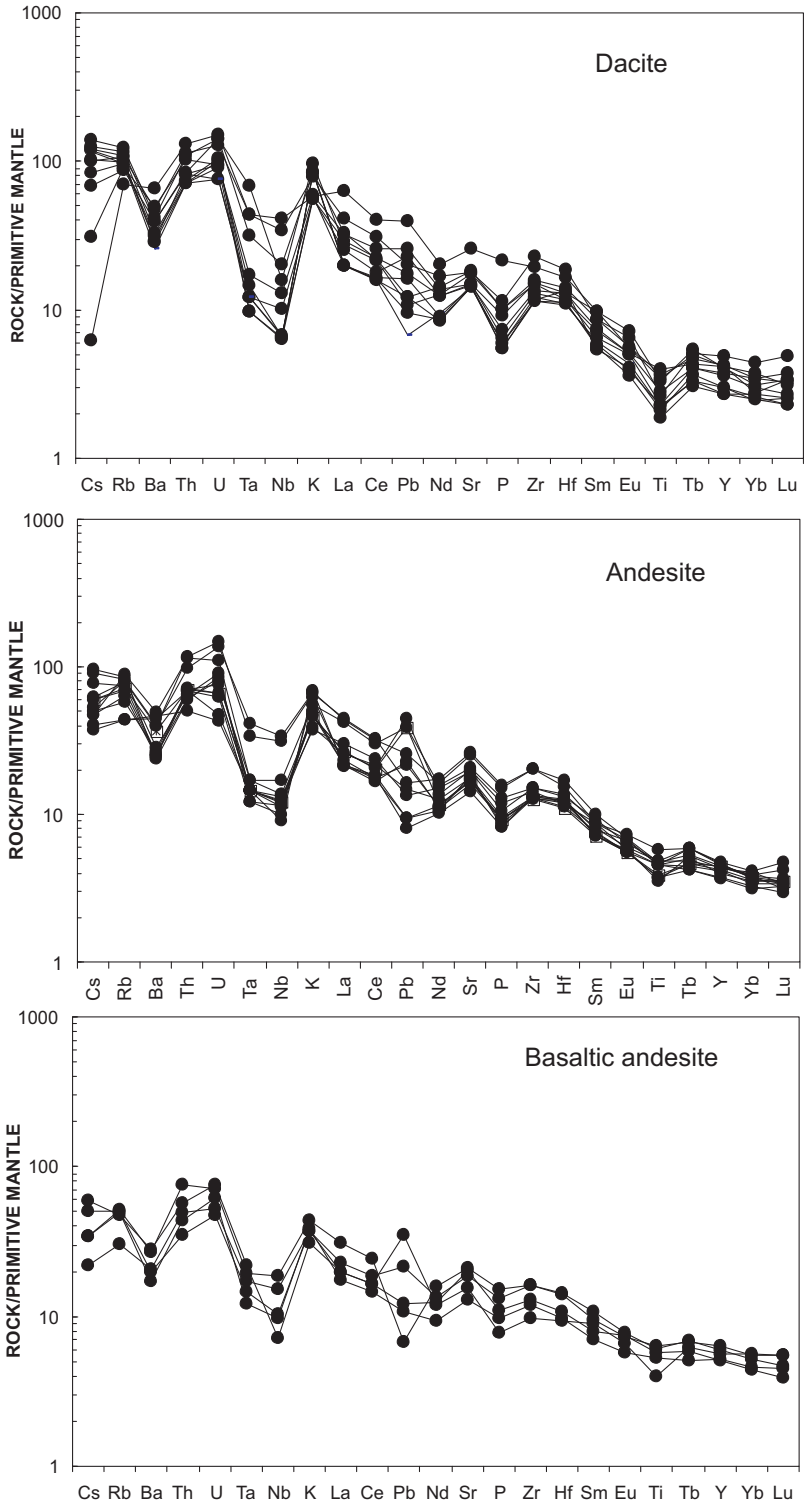

Figure 8. Primitive mantle normalized basaltic andesite, andesite and dacite patterns for the Yamadağı volcanics (normalized values from Sun & McDonough 1989).

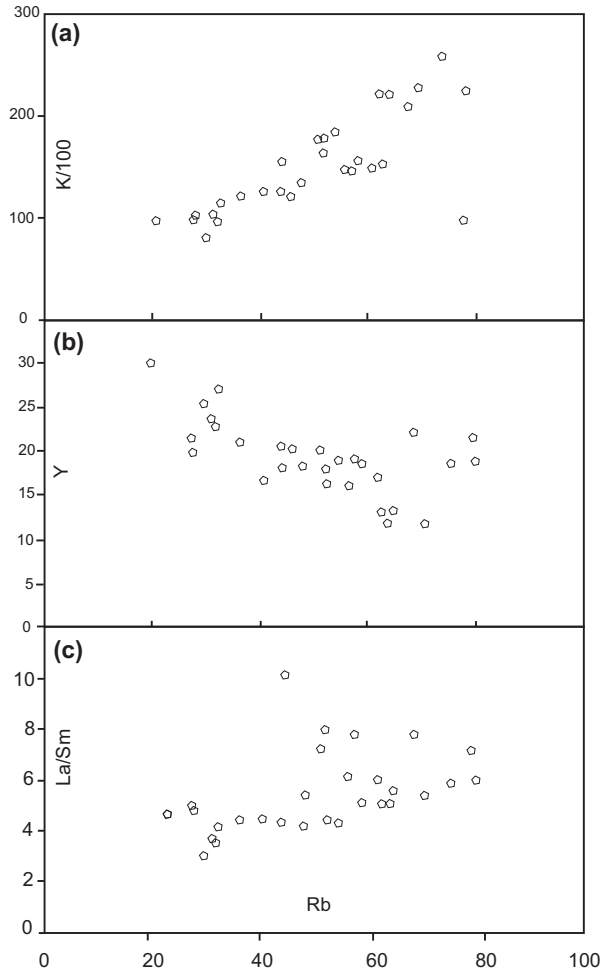

Figure 9. Some incompatible elements variations against Rb for the Yamadağı volcanics.

large increases in K_2O compared with smaller increases in K_2O/MgO and decreases in MgO. In contrast, contamination of magmas with crustal melts produces trajectories with low slopes on such plots. Figure 11 illustrates a plot of K_2O-K_2O/MgO for the Yamadağı volcanic, and shows these calc-alkaline rocks defining a low angle trajectory, which implies that the compositions of all the volcanics were affected by crustal interaction and so none can be assumed to be direct uncontaminated differentiates of primary mantle-derived magmas.

Magma Mixing

Petrographic data provide evidence for magma mixing in the Yamadağı volcanics. All rocks contain

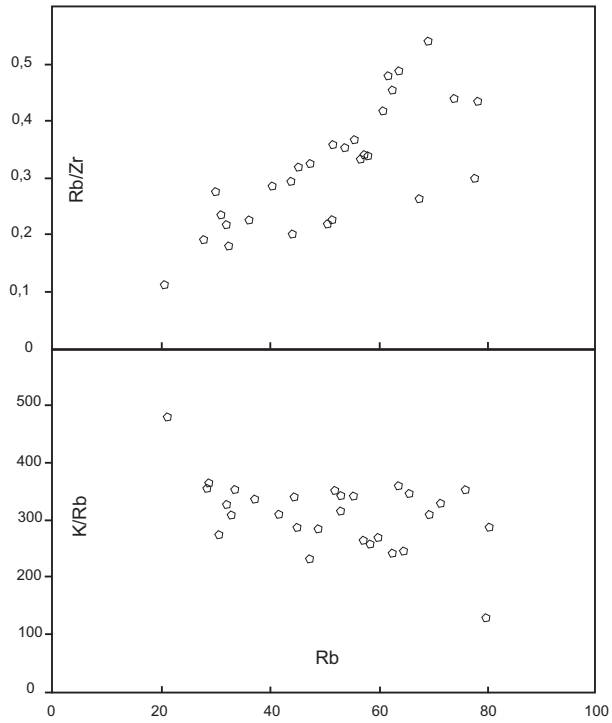

Figure 10. **(a)** Rb/Zr and **(b)** K/Rb variations against Rb for the Yamadağı volcanics.

disequilibrium mineral textures such as sieve-textured plagioclases, resorption of the ferromagnesian phases such as olivine, pyroxene and hornblende. Fine-grained resorption zones in plagioclase are probably caused by superheating, as described by Tsuchiyama (1985). The clear overgrowth rims on the sieved cores demonstrate that the reaction took place before crystallization of the inclusion groundmass began. Phenocrysts which are reacted and resorbed in the Yamadağı volcanics formed when their host magma interacted with a more basic one.

The Yamadağı volcanics contain both clinopyroxene and orthopyroxene. In some andesite samples, clinopyroxene is surrounded by a thin orthopyroxene rim (Figure 4D), possibly showing that both pyroxene types originated from different end members.

Hornblende phenocrysts within the Yamadağı volcanics have quite a different origin. Since hornblende in the dacitic member of the Yamadağı volcanics has a light green to green pleochroism, and

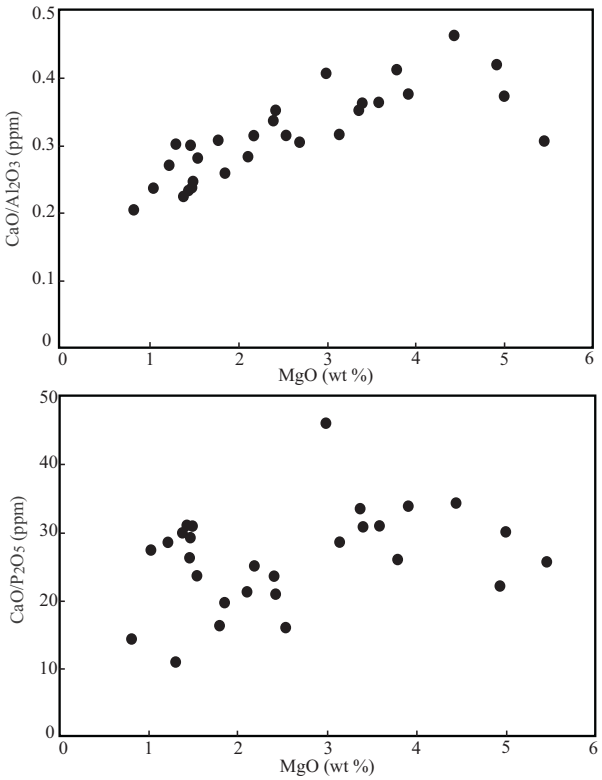

Figure 11. CaO/Al_2O_3 and CaO/P_2O_5 diagrams for Yamadağı volcanics.

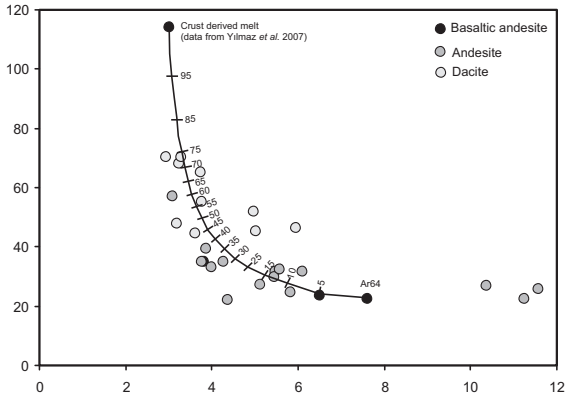

Figure 12. Trace element ratio/ratio diagram testing the validity of the mixing origin of the andesitic magmas of the Yamadağı volcanics.

that in the basaltic andesite and andesite has yellowish-brown to reddish-brown pleochroism, hornblende phenocrysts within the Yamadağı volcanics probably had at least two different origins.

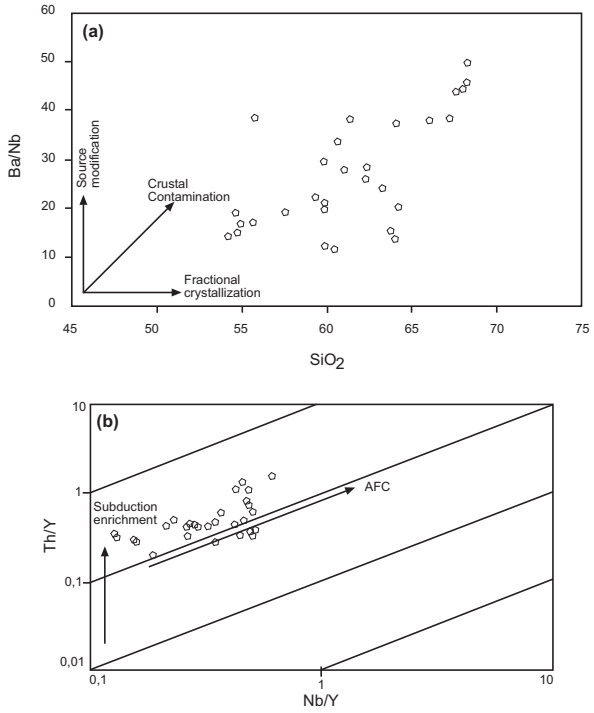

Figure 13. **(a)** Ba/Nb-SiO_2 and **(b)** Th/Y-Nb/Y diagrams for the Yamadağı volcanics.

One is a basaltic andesitic origin, as indicated by the presence of hornblende in the basaltic andesites and andesites whereas the other is a dacitic origin demonstrated by the presence of hornblende in the dacitic rocks. Yellowish-brown to reddish-brown rounded hornblendes mantled by resorption zones possibly indicate a xenocrystic origin within the Yamadağı volcanics.

Figure 12 tests the validity of mixing origin of the andesitic and dacitic rocks of the Yamadağı volcanics using a ratio/ratio diagram based on trace element data. In Figure 12, andesitic and dacitic rocks, except for three andesitic samples, fall on or near the hyperbolic mixing curve between basic magma derived from the mantle (basaltic andesite) and acidic magma derived from continental crust (data from Yılmaz *et al.* 1998).

Source Characteristics

Depletions of HFSE and enrichments of LILE relative to neighbouring elements in diagrams such as Figure 8 are widely considered diagnostic of

magmas generated from subduction processes (e.g., Thirwall *et al.* 1994 and references therein). However, magmas contaminated by continental crust also have depletions of HFSE and enrichments of LILE as continental crust is depleted in HFSE relative to LILE (Weaver & Tarney 1984; Taylor & McLennan 1985; Wilson 1989; Winter 2001). To address the problem whether the elevated LILE/HFSE ratios in the Yamadağı calc-alkaline volcanics reflect that of the source or crustal contamination, or both, Figure 13a plots Ba/Nb ratios of the Yamadağı volcanics against SiO_2. For the suite as a whole, Ba/Nb ratios increase as a function of differentiation. We consider these relationships to indicate that the Yamadağı volcanics have assimilated crustal material.

A Th/Y – Nb/Y plot (Figure 13b) provides some useful constraints concerning the different source components which may be involved in the petrogenesis of the magmas (Wilson *et al.* 1997). Samples from the Yamadağı volcanics define a coherent trend, with a Th/Nb ratio close to 0.1, which may be attributed to the combined effects of crustal assimilation and fractional crystallisation i.e.,.AFC. The displacement of this data array to higher Th/Y ratios than those of the oceanic basalt array (MORB and OIB) is strongly indicative of the metasomatism of the mantle source by subduction zone fluids carrying the trace element signature of a crustal component.

The subduction-related geochemical characteristics are therefore probably inherited from mantle lithosphere modified by slab fluids released during northward subduction of the Afro-Arabian plate beneath the Eurasian plate during Eocene to Miocene times (e.g., Pearce *et al.* 1990).

Conclusions

1. The Yamadagı volcanic rocks range from basaltic andesite to dacite and show a typical calc-alkaline differentiation trend.
2. Major- and trace-element variations indicate fractional crystallization.
3. Tectonic discrimination diagrams indicate that the mafic samples of the serie fall in to the calc-alkaline basalt field and intermediate-acidic members have a syn-collisional character.
4. HFSE depletions and LILE enrichments on the primitive mantle normalized trace element patterns imply that the magmas were derived from a mantle domain enriched by earlier subduction processes or assimilation of continental crust.
5. Disequilibrium mineral textures within the Yamadağı volcanics and incompatible element ratio plots imply that magma mixing is an important process on their evolution.
6. The variable characteristics of this collision-zone magmatism seem to have developed as a result of the superimposition of geotectonic settings, such as continent-continent collision, with a four-stage process (Harris *et al.* 1986). Therefore, the genesis of the Yamadağı volcanics can be attributed to complex petrogenetic processes, including partial melting of a metasomatized mantle, crystal fractionation, magma mixing, and assimilation of crustal materials along with fractional crystallization.

References

Allegre, C.J. & Minster, J.F. 1978. Quantitative models of trace element behaviour in magnetic processes. *Earth and Planetary Science Letters* **38**, 1–25.

Alpaslan, M. 1987. *Mineralogical and Petrographical Features of the Neogene Volcanics around Arguvan (NW Malatya).* MSc Thesis, Cumhuriyet University [unpublished].

Alpaslan, M. & Terzioğlu, N. 1996. Comparative geochemical features of the Upper Miocene and Pliocene volcanics around Arguvan (NW Malatya). *Geological Bulletin of Turkey* **39**, 75–86 [in Turkish with English abstract].

Balogh, K. 1985. K/Ar dating of Neogene volcanic activity in Hungary: experimental technique and methods of chronologic studies. *ATOMKI*, Report **D/1**, 277–288.

Bozkurt, E. 2001. Neotectonics of Turkey – a synthesis. *Geodynamica Acta* **14**, 3–30

Buket, E. & Temel, A. 1998. Major element, trace element, and Sr-Nd isotopic geochemistry and genesis of Varto (Muş) volcanic rocks, eastern Turkey. *Journal of Volcanological and Geothermal Research* **85**, 405–421.

Davidson, J.P., Ferguson, K.M., Colucci, M.T. & Dungan, M.A. 1987. The origin of magmas from the San Pedro-Pellado Volcanic Dokhan Volcanics Complex, S Chile: multicomponent sources and open system evolution. *Contribution to Mineralogy and Petrology* **100**, 429–445.

Dewey, J.F., Hempton, M.R., Kidd, W.S.F., Şaroğlu, F. & Şengör, A.M.C. 1986. Shortening of continental lithosphere: the neotectonics of Eastern Anatolia – a young collision Tectonics zone. *In*: Coward, M.P. & Riea, A.C. (eds), *Collision Tectonics*. Geological Society, London, Special Publications **19**, 3–36.

Ekİci, T. 2003. *Petrology of the Neogene Volcanics Along the Malatya Fault Between Arguvan and Arapkir (Malatya).* PhD Thesis, Çukurova Üniversity [unpublished].

Gülen, L. 1984. *Sr, Nd, Pb, Isotope and Trace Element Geochemistry of Calc-alkaline and Alkaline Volcanics, Eastern Turkey*. PhD Thesis, Massachusetts Instutue of Technology [unpublished].

Harris, N.B.W., Pearce, J.A. & Tindle, A.G. 1986. Geochemical characteristics of collision-zone magmatism. *In*: Coward, M.P. & Riea, A.C. (eds), *Collision Tectonics*. Geological Society, London, Special Publications **19**, 67–81.

Innocenti, F., Mazzuoli, R., Pasquare, G., Radicati Di Brozola, F. & Villari, L. 1976. Evolution of volcanism in the area of interaction between the Arabian, Anatolian and Iranian plates (Lake Van, Eastern Turkey). *Journal of Volcanology and Geothermal Research* **1**, 103–112.

Irvine, T.N. & Barager, W.R.A. 1971. A guide to the geochemical classification of the common volcanic rocks. *Canadian Journal of Earth Sciences* **8**, 523–548.

Keskİn, M., Pearce, J.A & Mitchell, J.G. 1998. Volcano-stratigraphy and geochemistry of collision-related volcanism on the Erzurum-Kars Plateou, Northern Turkey. *Journal of Volcanology and Geothermal Research* **85**, 355–404.

Koçyİğİt, A., Yilmaz A., Adamia S. & Kuloshvili, S. 2001. Neotectonics of East Anatolian Plateau (Turkey) and Lesser Caucasus: implication for transition from thrusting to strike-slip faulting. *Geodinamica Acta* **14**, 177–195.

Lambert, R.Stj., Holland, J.G. & Owen, P.F. 1974. Chemical petrology of a suite of calc-alkaline lavas from Mt. Ararat, Turkey. *Journal of Geology* **82**, 419–439.

Le Bas, M.J., Le Maitre, R.W., Streckeisen, A. & Zanettin, B. 1986. A chemical classification of volcanic rocks based on the total alkali-silica diagram. *Journal of Petrology* **27**, 745–750.

Le Maitre, R.W., Bateman, P., Dudek, A., Keller, J., Lameyre Le Bas, M.J., Sabine, P.A., Schmid, R., Sorensen, H., Streckeisen, A., Wolley, A.R., & Zonettin, B. 1989. *A Classification of Igneous Rocks and Glossory or Terms*. Blackwell, Oxford.

McKenzie, D.P. 1969. Plate tectonics of the Mediterranean region. *Nature* **220**, 239–343.

McKenzie, D. 1972. Active tectonics of the Mediterranean region. *Geophysical Journal of the Royal Astronomical Society* **30**, 109–185.

Notsu, K., Fujitani, T., Ui, T., Matsuda, J. & Ercan, T. 1995. Geochemical features of collision-related volcanics rocks in central and easthern Anatolia, Turkey. *Journal of Volcanology and Geothermal Research* **64**, 171–192.

Pearce, J.A. & Cann, J.R. 1973. Tectonic setting of basic volcanic rocks determined using trace element analyses. *Earth and Planetary Science Letters* **19**, 290–300.

Pearce, J.A., Bender, J.F., Delong, S.E., Kidd, W.S.F., Low, P.J., Güner, Y., Şaroğlu, F., Yilmaz, Y., Moorbath, S. & Mitchell, J.G. 1990. Genesis of collision volcanism in Eastern Anatolia, Turkey. *In*: Le Fort, P., Pearce, J.A. & Pecher, A. (eds), *Collision Magmatism*. Journal of Volcanology and Geothermal Research **44**, 189–229.

Peccerillo, A. & Taylor, S.R. 1976. Geochemistry of Eocene calc-alkaline volcanic rocks from the Kastamonu area, northern Turkey. *Contribution to Mineralogy and Petrology* **58**, 63–81.

Rutherford, M.J. & Hill, P.M. 1993. Magma ascent rates from amphibole breakdown: an experimental study applied to the 1980–1986 Mount St Helens eruptions. *Journal of Geophysical Research* **98**, 19667–19685.

Şaroğlu, F. & Yilmaz, Y. 1984. Doğu Anadolu'nun neotektoniği ile ilgili magmatizması [Magmatism related to the neotectonics of Eastern Anatolia]. *Ketin Symposium Proceeding*, 149–162 [in Turkish with an English abstract].

Şengör, A.M.C. 1980. *Principles of the Neotectonics of Turkey*. Geological Society of Turkey Publication no. **40**.

Şengör, A.M.C. & Kidd, W.S.F. 1979. Post-collisional tectonics of the Turkish-Iranian plateau and a comparison with Tibet. *Tectonophysics* **55**, 361–376.

Şengör, A.M.C. & Yilmaz, Y., 1981, Tethyan evolution of Turkey; a plate tectonic approach. *Tectonophysics* **75**, 181-241.

Şengör, A.M.C., Görür, N. & Şaroğlu, F. 1985. Strike-slip faulting and related basin formation in zones of tectonic escape: Turkey as a case study. *In*: Biddle, K,T. & Christie-Blick, N. (eds), *Strike-Slip Deformation, Basin Formation and Sedimentation*. Society of Economic, Paleontologists and Mineralogists, Special Publications **37**, 227–264.

Steiger, R.H. & Jager, E. 1977. Subcommission on geochronology: convention on the use of decay constants in geo- and cosmochronology. *Earth and Planetary Science Letters* **12**, 359–362.

Sun, S.S. & Mcdunough, W.F. 1989. Chemical and isotopic systematics of oceanic basalts: implications for mantle composition and processes. *In*: Saunders, A.D. & Norry, M.J. (eds), *Magmatism in Ocean Basins*. Geological Society, London, Special Publications **42**, 313–345

Taylor, S.R. & Mclennan, S.M. 1985. *The Continental Crust: its Composition and Evolution*. Blackwell Scientific Publications, Oxford, UK.

Thirlwall, M.F., Smith, T.E., Graham, A.M., Theodorou, N., Hollings, P., Davidson, J.P. & Arculus, R.D. 1994. High field strength element anomalies in arc lavas: source or processes. *Journal of Petrology* **35**, 819–838.

Tokel, S. 1984. Mechanism of crustal deformation in eastern Anatolia and the petrogenesis of young volcanites. *Ketin Symposium Proceedings*, 121–130 [in Turkish with and English abstract].

Tsuchiyama, A. 1985. Dissolution kinetics of plagioclase in the melt of the system diopside-albite-anorthite and origin of dusty plagioclase in andesites. *Contributions to Mineralogy and Petrology* **89**, 1–16.

Wilson, M. 1989. *Igneous Petrogenesis*. London Unwin Hyman.

Wilson, M., Tankut, A. & Güleç, N. 1997. Tertiary volcanism of the Galatia province, north-west Central Anatolia, Turkey. *Lithos* **42**, 105–121.

Winter, J.D. 2001. *An Introduction to Igneous and Metamorphic Petrology*. Prentice Hall.

Weaver, B. & Tarney, J. 1984. Empirical approach to estimating the composition of the continental crust. *Nature* **310**, 575–577.

Westaway, R. & Arger, J. 2001. Kinematics of the Malatya-Ovacık fault zone. *Geodynamica Acta* **14**, 103–131.

Yilmaz, Y. 1990. Comparison of young volcanic associations of western and eastern Anatolia formed under a compressional regime: a review. *Journal of Volcanology and Geothermal Research* **44**, 69–87.

Yilmaz, Y., Güner, Y. & Şaroğlu, F. 1998. Geology of the Quaternary volcanic centres of the east Anatolia. *Journal of Volcanology and Geothermal Research* **85**, 173–210.